

1 IMPROVING THE PROPERTIES OF HIGH VOLATILE COKING

2 COALS BY CONTROLLED MILD OXIDATION

3 M.F. Vega*, A.M. Fernández, E. Díaz-Faes, C. Barriocanal
4 Instituto Nacional del Carbón (INCAR-CSIC), Apdo 73, 33080 Oviedo. Spain

5 *Abstract*

6 Four bituminous coals of the same rank but with different thermoplastic properties were
7 oxidized at 40 and 50 °C for one month. The chemical changes due to oxidation were
8 studied by applying Gieseler plastometry, the free-swelling index (FSI),
9 thermogravimetric analysis and Fourier transform infrared spectroscopy (FTIR). In
10 general, oxidation at 50 °C produced a greater impairment of coking properties, the
11 different responses to oxidation depending on the parent coal. The main effects caused
12 by oxidation were a loss of thermoplastic properties, a decrease in aliphatic hydrogen
13 and a slight increase in groups with oxygen functionalities.

14 Both the fresh and oxidized coals were carbonized in a movable-wall oven of 17 kg
15 capacity and the quality of the resulting cokes was tested by means of the ASTM
16 standard method. The results showed that, in certain cases, mild oxidation produced an
17 improvement in coke quality. Oxidation also affected the porosity of the cokes, which
18 may be related to the coke quality. It was found that the higher quality cokes had less
19 macroporosity, whereas the lower quality cokes had a higher pore volume.

20 **Keywords:** *Bituminous coal, mild oxidation, thermoplasticity, coke quality, porosity*

21 **1. Introduction**

22 The natural oxidation of coal (weathering) occurs when the coal is still in the
23 seam (outcropping) and also during its transport and storage. The interaction of coal
24 with the atmosphere alters its physical properties and chemical composition [1,2]. It is
25 well known that oxidation leads to a gradual impairment of the fluid properties of coal
26 [3–6], which becomes more inert during the coking process with a consequent decrease
27 in coke quality and an increase in reactivity [7–9]. Because of this but also because
28 oxidation causes a reduction in coke yield, carbonization rate and coke productivity
29 [4,7,10], the oxidation of coal is a cause of great concern for the cokemaking industry.
30 Hence it is necessary to develop efficient methods to improve coke properties.

31 Although the oxidation of coal usually involves a reduction in coke quality,
32 some authors have observed the opposite effect in the initial stages of the process. It has
33 been established that, in certain cases, the mild oxidation of high volatile bituminous
34 coals can improve the strength of such cokes. Very high fluidity coals give rise to a
35 weak coke with a thin-walled porous structure. Mild oxidation reduces the fluidity of
36 such coals to an optimum value, which produces an improvement in their coking
37 properties [11,12]. The preheating of coals at temperatures of around 150 °C during an
38 optimum period of time leads to the incorporation of relatively small additional amounts
39 of oxygen into coals that are beneficial to coke strength [5]. On the other hand, slight
40 weathering improves the quality not only of cokes from high volatile coals but also of
41 those from medium and low volatile coals [13–15].

42 It is widely accepted that the development of thermoplasticity of coal particles
43 during coal carbonization is one of the key factors that determines the strength and
44 reactivity of the cokes formed [16]. Therefore, four high volatile bituminous coals with

45 different thermoplastic properties were selected for this work and oxidized at a low
46 temperature to simulate the weathering process.

47 Although metallurgical coke is produced from blends of coals it is necessary to
48 know how each single coal responds to oxidation. It should also be noted that the
49 behaviour of these coals might differ when they are part of a blend.

50 The principal aim of this study was to establish whether the mild oxidation of
51 coal would improve the quality of coke obtained from poor coking coals. To this end,
52 the chemical changes in the coals were followed by applying the Gieseler and free-
53 swelling index tests, thermogravimetric analysis and FTIR spectroscopy. The quality of
54 all the cokes obtained, and the porous texture of those that underwent more significant
55 variations in coke quality were examined in detail.

56 **2. Materials and methods**

57 *2.1 Coals*

58 The present work was carried out using four high volatile bituminous coals
59 (Table 1). The coals were placed on metal trays (64 cm length, 40 cm width and 3 cm
60 height). Oxidation was carried out in a drying chamber at 40 and 50 °C. Representative
61 samples were collected after 10, 20 and 30 days for carbonization. In the case of coal A
62 oxidation at 50 °C lasted up to 40 days. 30 oxidation days was found to be the most
63 suitable time for the mild oxidation of the remaining coals. The oxidized samples were
64 labelled with the letter of the corresponding coal followed by the temperature of
65 oxidation and the number of oxidation days.

66 Proximate analyses were performed following the ISO562 and ISO1171
67 standard procedures for volatile matter and ash content, respectively. The elemental
68 analysis was determined by means of a LECO CHN-2000 for C, H and N (ASTM D-

69 5773), a LECO S-144DR (ASTM D-5016) for sulphur and a LECO VTF-900 for the
70 direct determination of oxygen.

71 A petrographic examination of the samples was carried out on a MPV II Leitz
72 microscope by means of reflected white light using immersion objectives (32×) in
73 accordance with the ISO 7404-5 procedure for vitrinite reflectance and the ISO 7404-3
74 procedure to determine the maceral group.

75 *2.2 Ash analysis*

76 The total ash content of the coke samples was obtained by combustion of the
77 organic matter at 815 °C until constant mass, following the ISO 1171 (2010) standard
78 procedure. The concentrations of oxides (Al, Ca, Fe, K, Mg, Na, Si, P and Ti) were
79 determined using X-ray fluorescence spectroscopy (XRF). The XRF apparatus was a
80 sequential wavelength-dispersive Siemens SRS 3000 X-ray spectrometer equipped with
81 a Rh X-ray tube, a 58-position sample turntable, and a flow counter detector. Prior to
82 the XRF analysis the ashes obtained from the coke samples were subjected to a fusion
83 step using lithium tetraborate in order to obtain sample beads for analysis. The device
84 used to prepare the sample was a Philips Perl' X3 automatic fused bead machine.

85 *2.3 Thermoplastic properties*

86 The thermoplastic properties of the fresh and oxidized coals were assessed by
87 means of the free-swelling index (FSI) and the Gieseler fluidity tests. FSI was carried
88 out according to the ISO 501:2012 norm. This method consists in heating a sample of 1
89 g ($< 212 \mu\text{m}$) in a standard crucible for 2.5 min. The profile of the resulting coke is
90 compared to standard profiles. The Gieseler test was carried out in a R.B. Automazione
91 Gieseler plastometer PL 2000 following the ASTM D2639-08 standard procedure,
92 explained in detail in a previous paper [17].

93 *2.4 Thermogravimetric analysis (TG/DTG)*

94 The TG/DTG analysis of the pristine coals and oxidized samples was carried out
95 using a TA Instruments STD 2960 thermoanalyser. The samples (10 mg) with a particle
96 size of < 0.212 mm were heated to 1000 °C at a rate of 3 °C/min under a nitrogen flow
97 of 100 ml/min. From the data obtained by thermogravimetric analysis the volatile matter
98 evolved up to a specific temperature (VM_T) and the derivative weight loss curve (DTG
99 curve) were calculated. The volatile matter evolved over a specific temperature range
100 was calculated as the difference between the volatile matter evolved up to two specific
101 temperatures (VM_{T1-T2}). In addition, T_{max} , the temperature of maximum volatile matter
102 evolution, was derived from the TG/DTG curves [17,18].

103 *2.5 Fourier transform infrared spectroscopy (FTIR)*

104 Coal samples with a particle size of less than 0.063 mm were left to dry at 35 °C
105 overnight before analysis. The spectra of the pristine coals and oxidized samples were
106 measured using a collector diffuse reflectance accessory inserted into a Nicolet Magna-
107 IR560 spectrometer. A mercury cadmium telluride detector (MCT-A) that operates at a
108 sub ambient temperature was used. Data were collected in the range of 650 – 4000 cm^{-1} ,
109 by applying 128 scans at a resolution of 4 cm^{-1} to each sample. Semiquantitative
110 analyses were carried out using the integrated area (A) or the maximum intensity (H) of
111 the absorption bands to calculate selected indices.

112 *2.6 Carbonization test*

113 Carbonization tests of the fresh and oxidized coals were carried out in a movable
114 wall oven of approximately 17 kg capacity (MWO17). The dimensions of the oven are
115 250 mm L x 165 mm W x 790 mm H . A load cell was mounted on the movable wall to
116 measure the force exerted on the wall during carbonization. A programmable controller
117 was used to control the oven temperature. The temperature at the centre of the coal
118 charge was monitored by means of a thermocouple connected to a computer. The coal

119 was charged when the oven reached 1100 °C. The temperature of the wall was kept
120 constant throughout the test. The coke was pushed after reaching 3 h and 30 min when
121 the temperature in the centre of the charge was greater of 950 °C. As the bulk density
122 varies as a function of grain size and moisture content, both parameters were kept as
123 close as possible in each series of carbonizations to obtain a mean value of 770 ± 10
124 kg/m^3 on a dry basis.

125 *2.7 Coke quality*

126 The coke reactivity and mechanical strength after reaction were assessed by
127 means of the NSC test (ASTM D5341 standard procedure). A coke destined for use in
128 blast furnaces is required to have a CRI index value in the 20–30 % range and a CSR
129 index value above 60–65 % [19].

130 *2.8 Textural characterization*

131 The particle size selected to determine the porous structure of the cokes was
132 between 1 and 3 mm. The true density (ρ_{He}) of the coals and semicokes was measured
133 by means of helium pycnometry in a Micromeritics Accupyc 1330 Pycnometer. Their
134 apparent density (ρ_{Hg}) was determined with mercury at 0.1 MPa in a Micromeritics
135 autopore IV 9500 mercury porosimeter. From the true and apparent densities, the open
136 porosity corresponding to pore sizes of less than $12\mu\text{m}$ was calculated by means of the
137 following equation [20]:

$$\varepsilon(\%) = 1 - \frac{\rho_{\text{Hg}} (\text{g/cm}^3)}{\rho_{\text{He}} (\text{g/cm}^3)} \cdot 100$$

138 The total pore volume (V_{T}) was calculated from the equation:

$$V_{\text{T}}(\text{cm}^3/\text{g}) = \frac{1}{\rho_{\text{Hg}} (\text{g/cm}^3)} - \frac{1}{\rho_{\text{He}} (\text{g/cm}^3)}$$

139 The pore size distribution was obtained by applying increasing pressure to the
140 sample from 0.1 to 227 MPa which yielded pore sizes in the range of $12\mu\text{m}$ to 5.5 nm.

141 Pore size was classified into three categories, i.e. macropores ($12 \mu\text{m} > dp > 50 \text{ nm}$),
142 mesopores ($50 \text{ nm} > dp > 5.5 \text{ nm}$) and micropores ($dp < 5.5 \text{ nm}$). Microporosity was
143 calculated by difference relative to the total pore volume.

144 FE-SEM images were obtained on a Quanta FEG650 microscope (FEI Company) at 25
145 kV.

146 **3. Results and discussion**

147 [Table 1](#) shows the results of the proximate, ultimate and petrographic analyses of
148 the pristine coals. The coals are listed in order of increasing oxygen content. All the
149 coals are of the same rank, with a volatile matter content of around 31 wt. %, and
150 sulphur and ash contents of less than 0.93 and 10.5 wt. %, respectively, which is
151 characteristic of coals used for metallurgical coke production [19].

152 The maceral composition data in [Table 1](#) show that the American coals (A, B
153 and C) have a higher vitrinite (V) content with values ranging from 75.8 to 80.1 vol. %
154 mineral matter free (mmf) than Polish coal (D) that has a vitrinite content of 62.9 vol. %
155 mmf. The values of liptinite (L) range from 5.2 to 9.1 vol. % mmf. Semifusinite (SF)
156 and fusinite (F) represent the main components of the inertinite group. Also worth
157 noting is the high SF content of coal D (29.6 vol. % mmf).

158 Because the oxidation treatment was carried out in very mild conditions, no
159 significant changes were observed in the oxygen content of the coals. Only in the case
160 of coal A a slight increase was observed up to ca. 10 % for the A40-20 and A50-20
161 samples. Coal A was more affected by oxidation than coal B, which has the same origin
162 and composition, possibly because of its different petrographic characteristics. The
163 inertinite group maceral content in coal A was slightly higher than in coal B due to the
164 fact that these macerals are porous, which favours the diffusion of oxygen in the coal
165 mass [21]. This may explain the different responses of coals A and B to oxygen uptake.

166 Another possible explanation is their mineral matter content. It is known that
167 pyrite (FeS_2) is highly vulnerable to oxidation. The mechanism of pyrite oxidation has
168 been extensively studied and such oxidation invariably forms sulfuric acid as a by-
169 product [22–24]. Although mineral and maceral oxidations have been regarded in the
170 literature generally as more or less separate processes, it should be noted that the
171 acidification of the coal resulting from pyrite oxidation can catalyze and possibly
172 initiate the oxidation of C-H bonds in macerals into oxygen-bearing functional groups.
173 This implies that pyrite-rich coals can be expected to oxidize more readily than pyrite-
174 poor coals [25]. The mineral composition of coal is usually determined through its ash
175 content, where the mineral matter is present in the form of oxides. The percentages of
176 major-element oxides obtained by XRF analysis of the pristine coals, in relation to the
177 mass coal, are listed in [Table 2](#). The oxides with the highest percentages were Al_2O_3
178 (1.87 to 3.32 %) and SiO_2 (3.72 to 4.94 %) in addition to Fe_2O_3 (0.45 to 0.56 %). Since
179 coal A has a higher Fe_2O_3 and SO_3 content, it may also possible have a higher pyrite
180 content. In addition, Jiang Y. et al. attribute a high K ratio value, calculated as $(\text{Fe}_2\text{O}_3 +$
181 $\text{CaO} + \text{MgO})/(\text{SiO}_2 + \text{Al}_2\text{O}_3)$ to the presence of more iron-bearing minerals (siderite and
182 pyrite) in coals [26]. In the present study coals A and B give K ratio values of 0.14 and
183 0.10, respectively, which confirms the greater pyrite content of coal A.

184 *3.1 Variation of thermoplastic properties*

185 [Table 3](#) shows the parameters obtained from the Gieseler fluidity measurements
186 of the pristine coals. It can be see that the maximum fluidity (MF) values of the fresh
187 coals range from 3532 to 33328 ddp. Since the four coals have similar volatile matter
188 contents, the differences in their thermoplastic properties must be due to differences in
189 their maceral composition and oxygen content. The coals with the highest MF (A, B)
190 have the largest vitrinite and liptinite contents that are responsible for coal plasticity. On

191 the other hand coal D, which has the lowest MF (3532 ddpm), has the largest
192 semifusinite (SF) content (29.6 vol. % mmf). It is generally considered that two-thirds
193 of SF are inert during carbonization [19]. This, together with the fact that similar rank
194 coals which are richer in oxygen are less fusible, may explain the lower fluidity of coal
195 D compared to coals A, B and C.

196 Although, in general, the proximate and the ultimate analyses of the oxidized
197 coals did not show significant alterations, it is clear that the oxidation process produced
198 considerable changes in the plastic properties of the coals (Figure 1). It has been
199 established that the fixation of 0.1 % oxygen is enough to reduce plasticity appreciably
200 without causing significant impairment to other coking properties [27].

201 In order to facilitate comparison, loss of fluidity was expressed as a percentage
202 of the initial values. Figure 1 displays the variation of Gieseler maximum fluidity with
203 oxidation time at 40 and 50 °C. In general, the MF decreases to a greater extent with
204 oxidation at 50 °C, although each individual coal shows a different behaviour. The
205 highest MF loss is experienced by coal C that, after 30 oxidation days, loses around 78
206 % MF under either temperature. The decrease is more pronounced at 50 °C, where it
207 loses 52 % with respect to the initial value in just 10 oxidation days. Coals A and B
208 exhibit the most uniform fluidity loss at both temperatures, although the MF of coal B
209 barely diminishes 20 % after 30 oxidation days. Coal D maintains its MF during 10
210 oxidation days, after which it decreases promptly for 20 oxidation days. After that it
211 remains almost constant at around 30 and 50 % at 40 and 50 °C, respectively.

212 With regard to the other parameters derived from the Gieseler fluidity analysis no
213 significant variations were observed.

214 The free-swelling index values (FSI) of the pristine coals are collected in Table
215 3. Variations in the FSI with oxidation time were also analyzed, but contrary to other

216 studies [11,12] no improvement was observed in this index with mild oxidation. The
217 results obtained are in agreement with those derived from the Gieseler analysis.
218 However the FSI test is not as sensitive as the Gieseler test, and so in certain cases it
219 was unable to detect oxidation. For this reason the FSI value of coal A shows no
220 variation after oxidation at 40 °C, whereas it decreases from 7 to 5 1/2 after only 10
221 oxidation days at 50 °C. Coals B and C show no variation in FSI under any oxidation
222 temperature but for coal D it decreases by 1 point under both oxidation conditions.

223 3.2 Thermogravimetric analysis

224 The main parameters derived from the thermogravimetric analysis of the fresh
225 coals are presented in [Table 4](#). The evolution of the volatiles of the four coals is
226 dependent on their rank [18]. Only in the case of coal A were significant differences
227 observed between the fresh coal and the oxidized samples. The evolution of volatile
228 matter after oxidation occurs at a slower rate, decreasing at around 14 % under either
229 oxidation temperature. The diminution of the DTGmax with oxidation at 40 °C is
230 progressive, whereas at 50 °C it decreases sharply for 10 oxidation days, after which the
231 decrease is more moderate. It has been established that the loss of aliphatic moieties and
232 the formation of groups with oxygen functionalities reduce both the release of volatile
233 matter and the maximum rate of decomposition [28,29]. Molecular species released by
234 pyrolysis at ca. 400 °C contribute to the fluid phase. The depletion of these species leads
235 to an impairment of fluidity, which is reflected in the linear relationship between the
236 volatile matter released in the temperature range of 400 and 500 °C (VM400–500) and
237 the drop in the Gieseler maximum fluidity of the oxidized samples at 40 and 50 °C ([Fig.](#)
238 [2](#)). It can be seen that the lower the VM400–500 value is, the greater the decrease in the
239 thermoplastic properties of the oxidized samples. As expected, at 50 °C the decrease in
240 volatile matter evolved between 400 and 500 °C is greater than after oxidation at 40 °C.

241 3.3 FTIR spectroscopy of pristine coals and oxidized samples

242 Fresh coals and their oxidized samples treated for 30 days at 40 °C and 50 °C
243 were subjected to DRIFT analysis (the spectra of coal C are shown as an example in
244 Fig. S1). The main absorption bands that appear in the spectra of the four pristine coals
245 are identical: the broad absorption band with a maximum centred near 3300 cm⁻¹ is
246 assigned to OH groups. The range between 3100 and 2990 cm⁻¹ is associated to
247 stretching aromatic C–H. The range between 2990 and 2795 cm⁻¹ is assigned to
248 stretching aliphatic C–H and the range between 1750 and 1538 cm⁻¹ corresponds to the
249 C=O and C=C stretching modes. The 1600 cm⁻¹ band is assigned to the C=C stretching
250 vibrations of aromatic rings. The 900–700 cm⁻¹ range corresponds to out-of-plane
251 aromatic C–H vibration modes. From a qualitative point of view, no clear evidence of
252 mild oxidation was detected by DRIFT: the absorption bands corresponding to oxygen
253 functional groups remain unaltered in the spectra of the oxidized samples. Nor were any
254 changes observed in the intensity of the absorption bands associated to aliphatic and
255 aromatic hydrogens (Fig. S1).

256 In order to obtain a better knowledge of the structural modifications of the
257 oxidized coals as a function of time and temperature, a semi-quantitative analysis was
258 carried out. To this end, three indices were considered: (i) the H₃₀₄₀/H₂₉₂₀, ratio of the
259 height of the bands centred around 3040 and 2920 cm⁻¹, corresponding to aromatic and
260 aliphatic stretching vibrations, respectively, (ii) the A₁₄₄₅/A₁₃₇₅, ratio between the area
261 under the bands centred near 1445 and 1375 cm⁻¹ due to methylene and methyl groups
262 [6] and (iii) the CO/Car, ratio of the oxygen-containing structures to the aromatic carbon
263 content, which is defined as the ratio between the area under the bands in the region
264 between 1750-1640 cm⁻¹ and the area under the band centred near 1620 cm⁻¹ [30].
265 Table 5 shows the evolution of these indices after 30 oxidation days at 40 and 50 °C.

266 Due to the very mild conditions employed in the study, as well as the small differences
267 in the temperatures selected, only minor changes were observed in the indices. It can be
268 seen that the H_{3040}/H_{2920} and CO/Car indices increase only slightly as a consequence of
269 oxidation. These variations signify an increase in aromatic hydrogens and groups with
270 oxygen functionalities, respectively. The decrease observed in the A_{1445}/A_{1375} ratio
271 indicates a decrease in methylene groups. [Figure 3](#) displays the relationship between the
272 A_{1445}/A_{1375} ratio and the drop in fluidity. In general, the lower this index is, the higher
273 the fluidity loss. These results are in agreement with those obtained from the
274 thermogravimetric analysis. As has been established by Álvarez et al. in a previous
275 research study, decrease in aliphatic hydrogens, a decrease in methylene groups and the
276 probable formation of oxygen functionalities seem to be the factors that determine the
277 decrease in fluidity due to oxidation [6].

278 *3.4 Coke quality*

279 The quality parameters of the cokes produced from pristine coals are collected in
280 [Table 6](#). Coke D has the worst quality of the cokes derived from the pristine coals.
281 Although all the coals studied have the same rank the CRI index depends on various
282 factors such as coal rank, thermoplastic properties, the composition of the coal ash and
283 maceral composition [19]. It has been established that a high inertinite content (≥ 30
284 vol. %) in the parent coal increases the reactivity and reduces the strength of the
285 resultant coke [31]. In the present study coal D has the highest inertinite content (29.6
286 vol. % mmf) which may explain, at least partially, its higher CRI value with respect to
287 the other coals. However, ash composition can also influence the CRI/CSR value due to
288 the accelerating or inhibiting effect that certain minerals on coke gasification as a result
289 of catalytic reactions. Coal D has the highest percentage of basic oxides (Fe_2O_3 , CaO,
290 K_2O and Na_2O), which may also explain its low CSR value (44.9) [19].

291 The evolution of the DI_{15}^{150} index of the cokes with oxidation time is displayed in
292 [Figure 4](#). The trends observed differ depending on the original coal. In the case of coal
293 A, oxidation at 40 °C produces a gradual increase in cold mechanical strength up to 20
294 oxidation days, after which it returns to its initial value. During the first 20 oxidation
295 days at 50 °C the JIS index remains almost constant, but after 40 oxidation days it
296 decreases significantly. The mechanical strength of cokes produced from coals B and C
297 do not present any appreciable variations over the period of time studied. In the case of
298 cokes D, the JIS index experiences severe impairment at both oxidation temperatures.

299 [Figures 5](#) and [6](#) show the variation in CRI and CSR indices with oxidation time.
300 Coke A50-10 undergoes a very slight decrease in its CRI value and then, an increase in
301 its CSR index. However, in cokes B the CRI/CSR indices remain constant during 10
302 oxidation days at 40 °C after which they deteriorate progressively under both oxidation
303 temperatures. In cokes C the tendency depends on the oxidation temperature. At 40 °C
304 CRI decreases slightly, whereas CSR remains close to its initial value. However at 50
305 °C it goes through a maximum during 10 oxidation days after which it decreases to
306 values close to the initial value. In cokes D, CRI remains almost constant at 40 °C but at
307 50 °C tends to decrease after 10 oxidation days. The CSR values of D40-20 and D40-30
308 remain close to their initial value but they deteriorate at 50 °C.

309 To sum up, 20 oxidation days at 40 °C and 10 oxidation days at 50 °C improved
310 the quality of cokes derived from the coal with highest MF (A), whereas the quality of
311 cokes derived from coal B, with similar characteristics to coal A, remained almost
312 constant. The difference in both cases was a loss of thermoplastic properties in coal A as
313 a consequence of the mild oxidation treatment. This suggests that, as observed in
314 previous studies, a diminution in MF to a more appropriate values, could be a way to
315 improve coke quality [12,32].

316 *3.5 Cokes porous texture*

317 SEM images were taken in order to assess the qualitative changes in the porous
318 macropore structure of cokes produced from fresh coal A and its oxidized samples,
319 (Figure 7). The cokes which underwent the greatest changes in quality after oxidation
320 were selected for the study. Cokes A40-20 and A50-10, both of which showed an
321 improvement in quality with respect to the pristine coal, experienced a decrease in
322 macroporosity. These cokes are more compact and have a smaller pore size than the
323 coke obtained from the fresh coal A. Comparison also shows that A50-10 has a higher
324 pore wall thickness, a feature that makes this coke more consistent, which is in
325 agreement with the results derived from the NSC test. It follows that the enhancement in
326 mechanical strength of A40-20 and A50-10 may be related to the decrease in macropore
327 volume. With respect to coke A50-40, as expected, the increase in the volume of
328 macropores led to an impairment of its mechanical strength. These results are in
329 accordance with those derived from a previous research study [14] and indicate the
330 influence of porosity development on the quality of the resultant cokes.

331 In order to confirm the qualitative changes in the porous structure of the cokes
332 due to the different oxidation conditions, a porosity study of the cokes obtained from
333 coal A (A, A40-20, A50-10 and A50-40) was carried out. It is generally accepted that
334 the development of coke porous structure during the carbonization process depends
335 partly on the characteristics of parent coal (rank, fluidity) and partly on the conditions of
336 the process (bulk density, heating rate, etc...), whereas oxidation modifies the porous
337 structure and enhances the porosity of the resultant cokes [9,33].

338 The helium (true) and mercury (apparent) density, porosity and the total pore
339 volume values obtained from the characterization of the cokes are listed in Table 7.
340 Mercury porosimetry was used to evaluate the meso- and macro-porosity of the cokes.

341 Although the porosity measured only represents a fraction of the total porosity of the
342 cokes studied the trends observed were useful to explain the variations in quality of the
343 cokes A. The true and apparent densities of the cokes do not show significant
344 differences. Nevertheless a slight decrease in total pore volume and porosity is observed
345 in the A40-20 and A50-10 cokes. Small variations in pore size distribution are also
346 observed. The volume of macropores decreases in the case of A40-20 and A50-10
347 whereas it increases in A50-40. There is no significant variation in the volume of
348 mesopores.

349 **4. Conclusions**

350 The effect of mild oxidation on the characteristics of four coals of similar
351 volatile matter content was found to be different. Although oxidation did not produce
352 important variations in the oxygen content the thermoplastic properties were impaired.
353 Loss of fluidity was greater after oxidation at 50 °C. The petrographic characteristics of
354 the coals and their mineral matter composition seemed to determine the responses of the
355 four coals to mild oxidation. A decrease in maximum fluidity favored an enhancement
356 of coke quality. Oxidation of the coal with a MF of 16241 ddpm at 40 °C resulted in a
357 maintenance of coke quality, whereas the quality of the coke obtained from coal of the
358 lowest fluidity was impaired under all of the oxidation conditions. The total pore
359 volume and the porosity of the cokes derived from the highest fluidity coal decreased.
360 This was accompanied by a diminution in macropore volume, which yielded in cokes
361 with a higher mechanical strength.

362 *Acknowledgements*

363 The research leading to these results has received funding from the European Union's
364 Research Programme of the Research Fund for Coal and Steel (RFCS) research
365 programme under grant agreement No. [RFCR-CT-2013-00007]. We also thank Dr.

366 Łukasz Smędowski from Instytut Chemicznej Przeróbki Węgla (Poland) for supplying
367 coal D used for this research.

- [1] C. R. Nelson. Chemistry of coal weathering, Coal Science and Technology. vol. 14. Amsterdam: Elsevier; 1989.
- [2] Pisupati SV, Scaroni AW. Natural weathering and laboratory oxidation of bituminous coals: Organic and inorganic structural changes. Fuel 1993;72:531–42. doi:10.1016/0016-2361(93)90113-G.
- [3] Wu MM, Robbins GA, Winschel RA, Burke FP. Low-temperature coal weathering: its chemical nature and effects on coal properties. Energy Fuels 1988;2:150–7.
- [4] H.S. Valia. Effects of coal oxidation on coke making. ISS-Ironmak. Conf. Proc, vol. 49, Detroit: Iron And Steel Society; 1990, p. 199–209.
- [5] Seki H, Ito O, Iino M. Effect of mild oxidation of bituminous coals on caking properties. Fuel 1990;69:317–21. doi:10.1016/0016-2361(90)90093-6.
- [6] Casal MD, González AI, Canga CS, Barriocanal C, Pis JJ, Alvarez R, Díez MA. Modifications of coking coal and metallurgical coke properties induced by coal weathering. Fuel Process Technol 2003;84:47–62. doi:10.1016/S0378-3820(03)00045-6.
- [7] Crelling JC, Schrader RH, Benedict LG. Effects of weathered coal on coking properties and coke quality. Fuel 1979;58:542–6. doi:10.1016/0016-2361(79)90175-3.
- [8] Pis JJ, Cagigas A, Simón P, Lorenzana JJ. Effect of aerial oxidation of coking coals on the technological properties of the resulting cokes. Fuel Process Technol 1988;20:307–16. doi:10.1016/0378-3820(88)90029-X.
- [9] Cimadevilla JLG, Álvarez R, Pis JJ. Effect of coal weathering on technological properties of cokes produced at different scales. Fuel Process Technol 2005;86:809–30. doi:10.1016/j.fuproc.2004.08.002.

- [10] Miroshnichenko DV, Drozdnik ID, Kaftan YS, Bidolenko NB, Desna NA. Coking of coal batch with different content of oxidized coal. *Coke Chem* 2012;55:155–64. doi:10.3103/S1068364X12050067.
- [11] B. Ignasiak, D. Carson, P. Jadernik, N. Berkowitz. Metallurgical cokes from oxidized highly caking coals. *CIM Bulletin* 1979;72:154.
- [12] Sarkar S. Effect of weathering on caking and coking properties of coal. *Fuel* 1980;59:450–1. doi:10.1016/0016-2361(80)90206-9.
- [13] Alvarez R, Barriocanal C, Casal MD, Díez MA, Cimadevilla JLG, Pis JJ, Canga CS. Weathering Study of an Industrial Coal Blend Used in Cokemaking. *ISIJ Int* 1998;38:1332–8.
- [14] Álvarez R, Cimadevilla JLG, Barriocanal C, Casal MD, Díez MA, Pis JJ, Canga CS. Influence of coal weathering on coke quality. *Ironmak Steelmak* 2003;30:307–12.
- [15] Smędowski Ł, Piechaczek M. Impact of weathering on coal properties and evolution of coke quality described by optical and mechanical parameters. *Int J Coal Geol* n.d. doi:10.1016/j.coal.2016.08.005.
- [16] Komaki I, Itagaki S, Miura T. *Structure and Thermoplasticity of Coal*. Nova Publishers; 2005.
- [17] Díaz-Faes E, Barriocanal C, Díez MA, Alvarez R. Characterization of different origin coking coals and their blends by Gieseler plasticity and TGA. *J Anal Appl Pyrolysis* 2007;80:203–8. doi:10.1016/j.jaap.2007.02.008.
- [18] Barriocanal C, Díez MA, Alvarez R, Casal MD, Canga CS. On the relationship between coal plasticity and thermogravimetric analysis. *J Anal Appl Pyrolysis* 2003;67:23–40. doi:10.1016/S0165-2370(02)00012-8.

- [19] Díez MA, Alvarez R, Barriocanal C. Coal for metallurgical coke production: predictions of coke quality and future requirements for cokemaking. *International Journal of Coal Geology* 2002;50:389–412. doi:10.1016/S0166-5162(02)00123-4.
- [20] Krzesińska M, Pusz S, Smędowski Ł. Characterization of the porous structure of cokes produced from the blends of three Polish bituminous coking coals. *Int J Coal Geol* 2009;78:169–76. doi:10.1016/j.coal.2008.11.002.
- [21] Misra BK, Singh BD. Susceptibility to spontaneous combustion of Indian coals and lignites: an organic petrographic autopsy. *Int J Coal Geol* 1994;25:265–86. doi:10.1016/0166-5162(94)90019-1.
- [22] Huggins F., Huffman G., Lin M. Observations on low-temperature oxidation of minerals in bituminous coals. *Int J Coal Geol* 1983;3:157–82. doi:10.1016/0166-5162(83)90008-3.
- [23] Wang H, Dlugogorski BZ, Kennedy EM. Analysis of the mechanism of the low-temperature oxidation of coal. *Combust Flame* 2003;134:107–17. doi:10.1016/S0010-2180(03)00086-5.
- [24] Jerz JK, Rimstidt JD. Pyrite oxidation in moist air1. *Geochim Cosmochim Acta* 2004;68:701–14. doi:10.1016/S0016-7037(03)00499-X.
- [25] Huggins FE, Huffman GP, Dunmyre GR, Nardozzt MJ, Lin MC. Low-temperature oxidation of bituminous coal: Its detection and effect on coal conversion. *Coal Characterisation Convers Process* 1987;15:233–44. doi:10.1016/0378-3820(87)90048-8.
- [26] Jiang Y, Zhao L, Zhou G, Wang X, Zhao L, Wei J, Song H. Petrological, mineralogical, and geochemical compositions of Early Jurassic coals in the Yining Coalfield, Xinjiang, China. *31st Annu Meet TSOP* 2015;152, Part A:47–67. doi:10.1016/j.coal.2015.07.011.

- [27] Loison R, Foch P, Boyer A. *Coke: Quality and Production*. London: Elsevier; 1989.
- [28] Pisupati SV, Scaroni AW, Hatcher PG. Devolatilization behaviour of naturally weathered and laboratory oxidized bituminous coals. *Fuel* 1993;72:165–73. doi:10.1016/0016-2361(93)90393-G.
- [29] De La Puente G, Iglesias MJ, Fuente E, Pis JJ. Changes in the structure of coals of different rank due to oxidation - Effects on pyrolysis behaviour. *J Anal Appl Pyrolysis* 1998;47:33–42.
- [30] Ibarra JV, Miranda JL. Detection of weathering in stockpiled coals by Fourier transform infrared spectroscopy. *Vib Spectrosc* 1996;10:311–8. doi:10.1016/0924-2031(95)00060-7.
- [31] Pusz S, Buszko R. Reflectance parameters of cokes in relation to their reactivity index (CRI) and the strength after reaction (CSR), from coals of the Upper Silesian Coal Basin, Poland. *Int J Coal Geol* 2012;90–91:43–9. doi:10.1016/j.coal.2011.10.008.
- [32] Álvarez, R, Barriocanal C, Casal MD, Díez MA, González AI, Pis JJ, Canga CS. Coal weathering studies. *Ironmak Conf Proc* 1996;55:265.
- [33] Pis JJ, Centeno TA, Mahamud M, Fuertes AB, Parra JB, Pajares JA, Bansal RC. Preparation of active carbons from coal part I. Oxidation of coal. *Fuel Process Technol* 1996;47:119–38. doi:10.1016/0378-3820(96)01003-X.

Table 1. Proximate, ultimate and petrographic analysis of the pristine coals.

Coals	A	B	C	D
Ash (wt. % db ^a)	7.1	6.7	8.7	10.5
Volatile matter (wt. % db ^a)	32.9	32.1	30.6	30.7
C (wt. % db ^a)	81.0	82.6	78.2	77.1
H (wt. % db ^a)	5.0	5.0	4.8	4.7
N (wt. % db ^a)	1.8	1.6	1.9	1.5
S (wt. % db ^a)	0.93	0.85	0.65	0.67
O (wt. % db ^a)	4.1	4.3	4.8	5.3
<i>Petrographic characteristics</i>				
Mean vitrinite reflectance, Ro (%)	1.00	0.97	1.04	0.97
Vitrinite (vol. % mmf ^b)	75.8	77.9	80.1	62.9
Liptinite (vol. % mmf ^b)	9.1	8.4	5.2	7.4
Fusinite (vol. % mmf ^b)	1.9	2.0	0.7	0.0
Semifusinite (vol. % mmf ^b)	8.7	8.0	14.1	29.6
Other inertinites (vol. % mmf ^b)	4.6	3.7	0.0	0.0

^a Dry basis

^b Mineral matter free

Table 2. Ash chemical composition (wt. %) of the coals as determined by XRF.

Coal	Na ₂ O	MgO	Al ₂ O ₃	SiO ₂	P ₂ O ₅	K ₂ O	CaO	TiO ₂	Fe ₂ O ₃	SO ₃
A	0.04	0.08	1.96	3.72	0.01	0.20	0.18	0.10	0.56	0.13
B	0.03	0.06	1.87	3.87	0.00	0.20	0.07	0.08	0.47	0.05
C	0.11	0.11	2.72	4.43	0.12	0.22	0.24	0.13	0.45	0.15
D	0.15	0.23	3.32	4.94	0.21	0.31	0.39	0.13	0.45	0.31

Table 3. Gieseler parameters of the pristine coals.

Coal	Ts (°C) ^a	Tf (°C) ^b	Tr (°C) ^c	Tr – Ts (°C) ^d	MF (ddpm) ^e	FSI
A	380	442	487	107	33328	7
B	386	428	491	105	27237	7
C	389	448	490	101	16241	7
D	400	444	484	84	3532	5 ^{1/2}

^a Softening temperature, defined as the temperature at which the stirrer starts to rotate.

^b Maximum fluidity temperature.

^c Resolidification temperature, defined as the temperature at which the stirrer stops.

^d Plastic range.

^e Maximum fluidity expressed in dial divisions per minute (ddpm).

Table 4. Parameters derived from the thermogravimetric analysis of the pristine coals performed at 3 °C/min.

	Ti (°C) ^a	Tf (°C) ^b	Tf-Ti	VM400 (%) ^c	VM400- 500 (%) ^c	VM500- 750 (%) ^c	DTGmax (%/min) ^d	Tmax (°C) ^e	CY (%) ^f
A	337	780	443	14.6	56.9	22.4	0.89	448	68.0
B	327	765	438	16.4	56.9	21.1	0.91	449	68.7
C	345	777	432	14.4	56.6	23.0	0.78	449	70.7
D	352	777	425	12.6	58.1	23.2	0.85	446	69.5

^a Temperature at 5 % conversion.

^b Temperature at 95 % conversion.

^c Volatile matter evolved up to a specific temperature (T) or in a specific temperature range and normalized to 100 %.

^d Maximum rate of volatile matter evolution.

^e Temperature of maximum volatile matter release.

^f Coke yield at 1000 °C.

Table 5. Evolution of the DRIFT indices^a for the pristine coals and samples oxidized for 30 days at 40 and 50 °C.

	H ₃₀₄₀ /H ₂₉₂₀	A ₁₄₄₅ /A ₁₃₇₅	CO/Car
A	0.28	4.45	0.40
A40-30	0.30	4.34	0.43
A50-40	0.29	4.34	0.49
B	0.27	4.34	0.47
B40-30	0.39	4.10	0.41
B50-30	0.49	3.96	0.49
C	0.27	4.40	0.39
C40-30	0.32	3.99	0.45
C50-30	0.31	3.97	0.51
D	0.26	4.64	0.38
D40-30	0.29	4.26	0.41
D50-30	0.29	3.99	0.46

^a See text for definitions.

Table 6. Quality parameters of the cokes produced from the pristine coals.

Cokes	DI150/5	DI150/15	CRI	CSR
A	14.7	76.1	28.2	52.7
B	19.2	71.2	22.2	54.3
C	16.6	75.4	23.1	56.1
D	22.9	68.2	31.9	44.9

Table 7. Evolution of the porous characteristics of the cokes produced from coal A^a.

Cokes	ρ_{He} (g/cm ³)	ρ_{Hg} (g/cm ³)	ε (vol. %)	V_{T} (mm ³ /g)	V_{macro} (mm ³ /g)	V_{meso} (mm ³ /g)	V_{micro} (mm ³ /g)
A	1.80	1.55	13.6	87.3	45.8	8.5	33.1
A40-20	1.76	1.56	11.3	72.3	39.1	7.1	26.0
A50-10	1.80	1.62	10.2	63.3	41.3	7.6	14.5
A50-40	1.77	1.54	13.0	85.6	49.7	9.0	25.9

^a Values are presented on a dry ash free basis. ρ_{He} : true density; ρ_{Hg} : apparent density; ε : porosity calculated by means of Eq. (1); V_{T} : total pore volume calculated by means of Eq. (2); V_{macro} : macropore volume; V_{meso} : mesopore volume; V_{micro} : micropore volume.

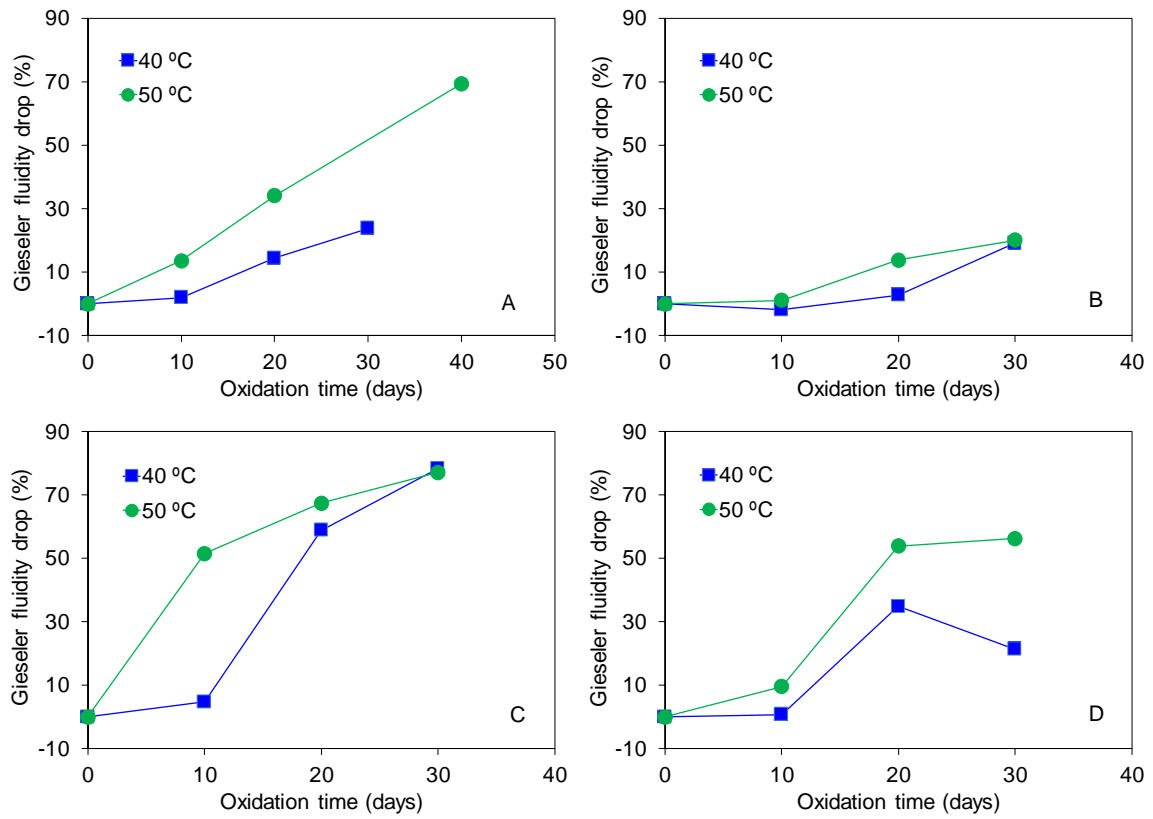


Figure 1. Decrease in the Gieseler fluidity of the oxidized samples at 40 and 50 °C.

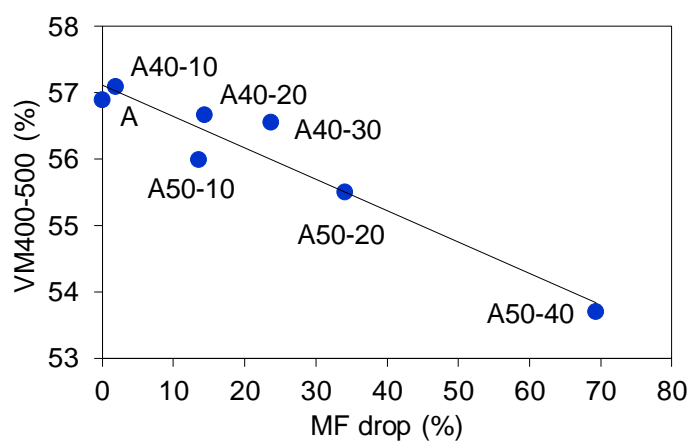


Figure 2. Relationship between the drop in Gieseler maximum fluidity and the volatile matter released in the temperature range between 400 and 500 °C (VM400–500).

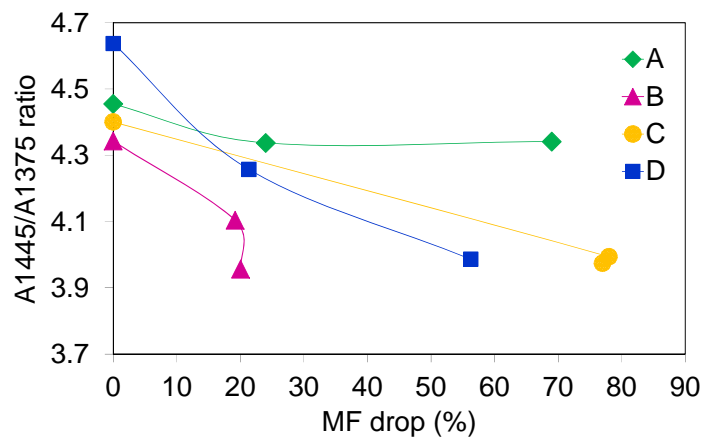


Figure 3. Variation in the ratio of the methylene to methyl groups with Gieseler maximum fluidity variation.

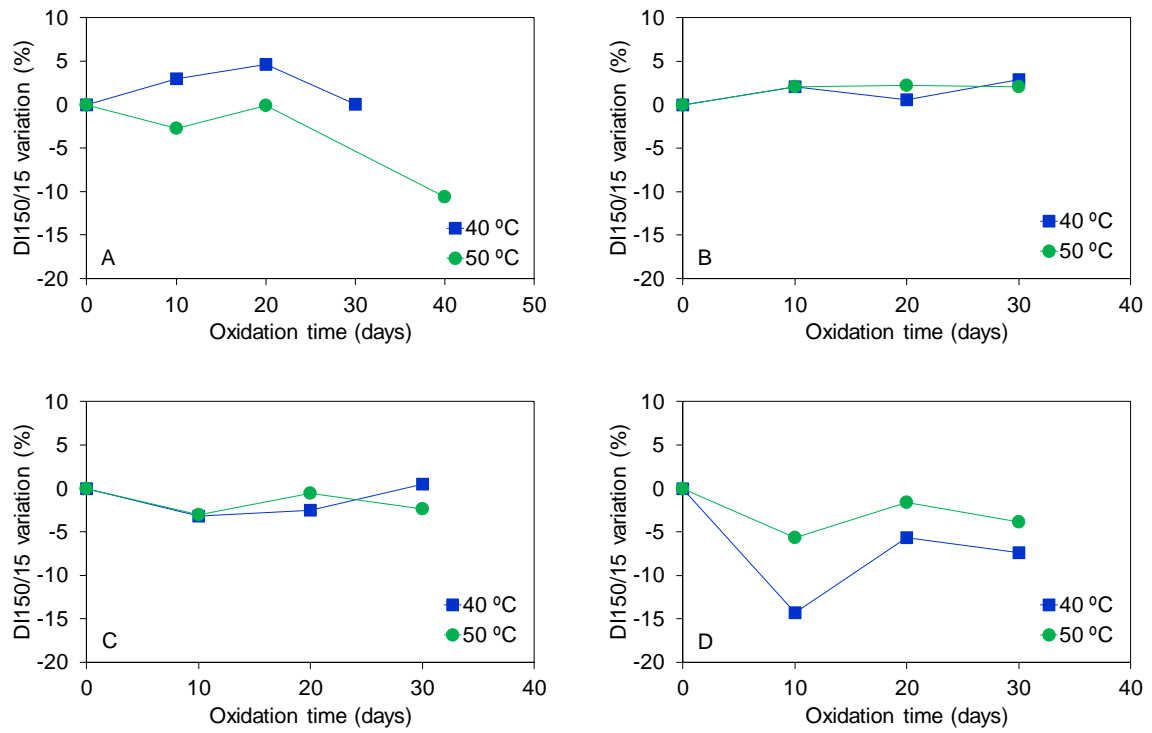


Figure 4. Variation of the mechanical strength of the oxidized samples at 40 and 50 °C with oxidation time.

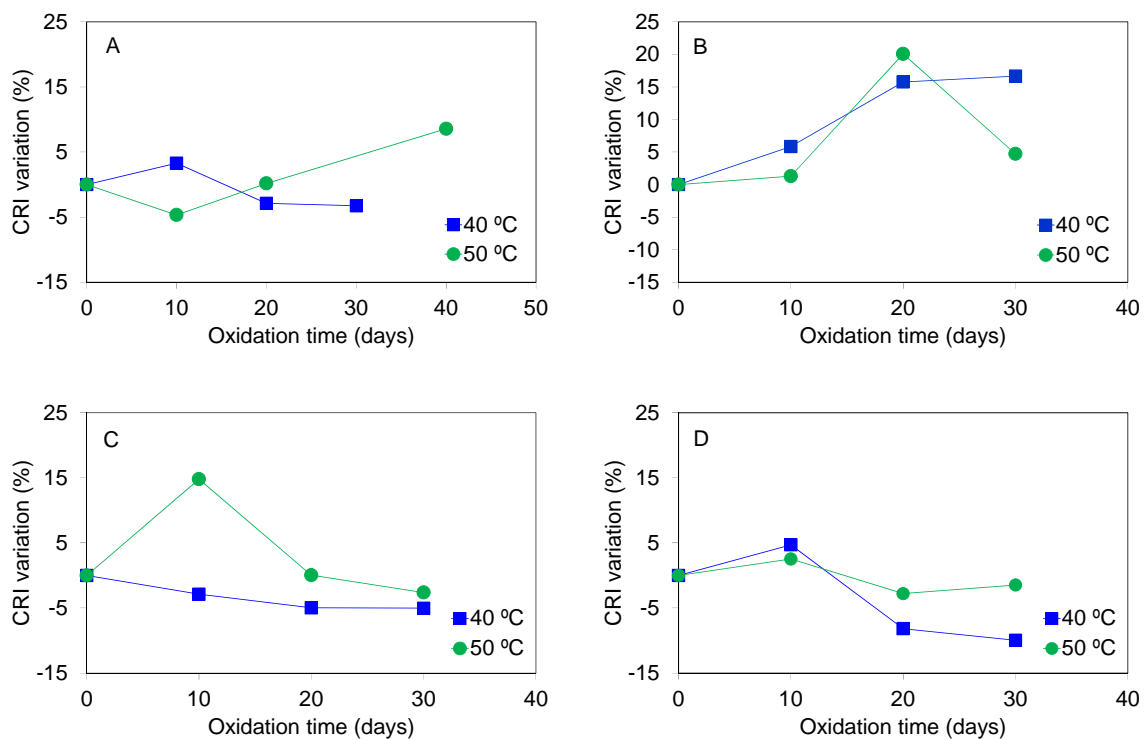


Figure 5. Variation of the coke reactivity of the oxidized samples at 40 and 50 °C with oxidation time.

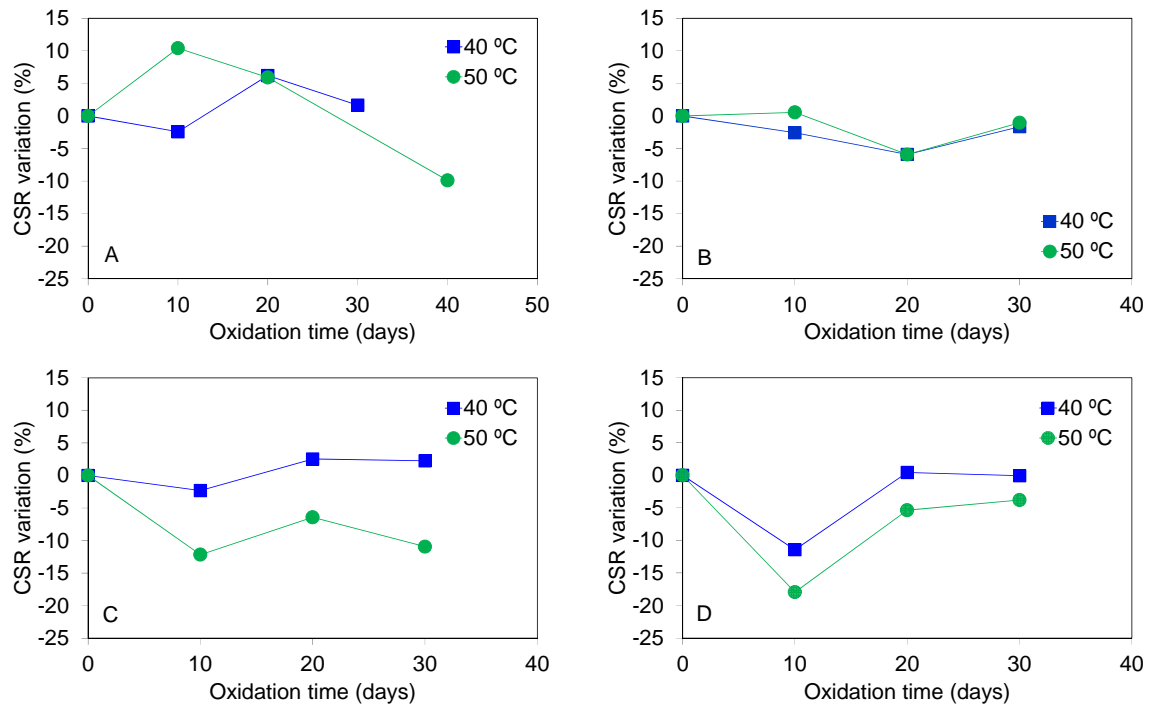


Figure 6. Variation of the CSR of the oxidized samples at 40 and 50 °C with oxidation time.

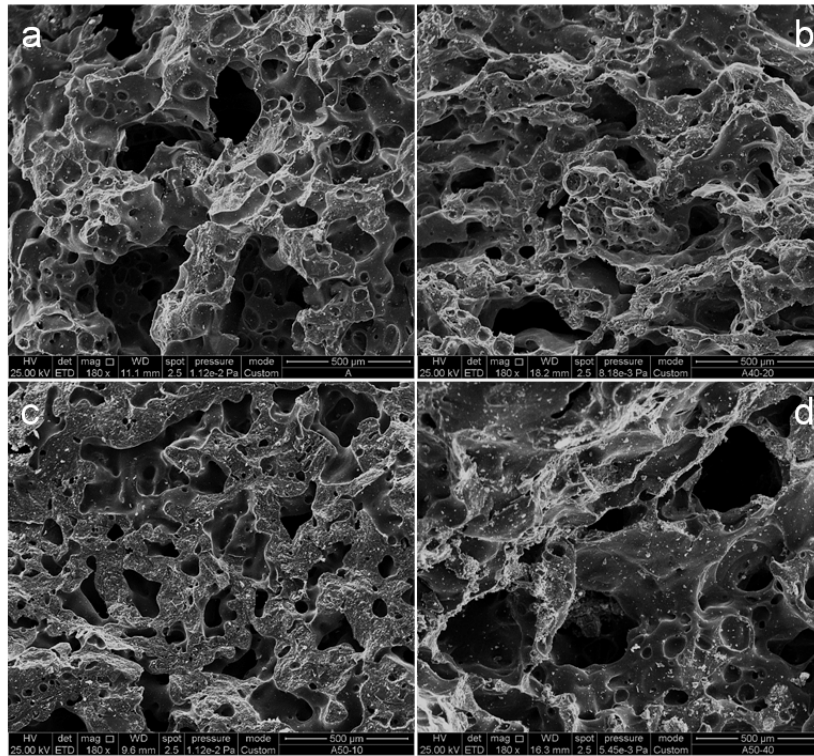


Figure 7. SEM images of the semicokes obtained from (a) A, (b) A40-20, (c) A50-10 and (d) A50-40.